

## The improvement of surface current of 2.6 $\mu\text{m}$ InGaAs photodetectors by using ICPCVD technology

Xiaoli Ji<sup>a</sup>, Baiqing Liu<sup>a</sup>, Hengjing Tang<sup>b,c</sup>, Xue Li<sup>b,c</sup>, Ming Shi<sup>b,c</sup>, Ying Zhou<sup>a</sup>,  
Yue Xu<sup>a</sup>, Haimei Gong<sup>b,c</sup> and Feng Yan<sup>a</sup>

<sup>a</sup>College of electronic science & engineering, Nanjing University, Nanjing 210093, China

<sup>b</sup>Key Laboratory of Infrared Imaging Materials and Devices, Shanghai Institute of Technical Physics, Chinese Academy of Sciences, Shanghai 200083, China

<sup>c</sup>State Key Laboratory of Transducer Technology, Shanghai Institute of Technical Physics, Chinese Academy of Sciences, Shanghai 200083, China

### Abstract

The surface leakage current has been studied for 2.6 $\mu\text{m}$  mesa InGaAs/InP p-i-n photodetectors by using ICPCVD and PECVD surface passivation technologies. It is found the dark current by using ICPCVD is significantly reduced comparing to PECVD due to the decrease of the device surface leakage current. A TCAD-based dark current model further reveals the dark current mechanism and the surface recombination current contributions in both ICPCVD and PECVD detectors.

### 1. Introduction

The extended wavelength  $\text{In}_x\text{Ga}_{1-x}\text{As}/\text{InP}$  photodetectors, which cover near infrared (NIR) range, have attracted much more attention due to their important application in environmental research, earth observation, special night vision, etc[1-2]. However, due both to the smaller band-gap and to defects from the bulk and surface, longer wavelength InGaAs detectors have considerably high dark currents [3]. In this paper, we use two various surface passivation technologies, Inductively Coupled Plasma Chemical Vapor Deposition (ICPCVD) and Plasma Enhanced Chemical Vapor Deposition (PECVD) technology to fabricate 2.6  $\mu\text{m}$  mesa InGaAs/InP p-i-n photodetectors[4]. We found that the dark current is significantly suppressed by using ICPCVD. A TCAD-based dark current model is constructed to reveal the surface leakage contributions in both ICPCVD and PECVD devices.

### 2. Experimental

2.6 $\mu\text{m}$  mesa  $\text{In}_{0.83}\text{Ga}_{0.17}\text{As}/\text{InP}$  p-i-n photo-detectors were fabricated by Gas Source Molecular Beam Epitaxy

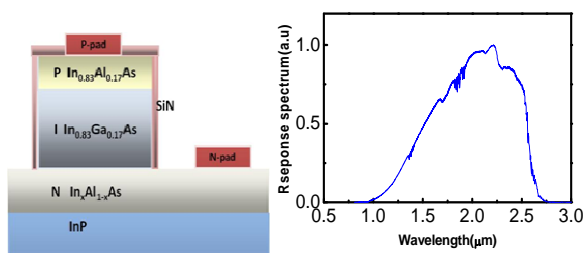


Fig.1 (a) The cross-section view of the detectors; (b) The normalized spectral response at room temperature for the detectors.

(GSMBE) technology on InP substrate [5]. The p-i-n structure consists of 1.9  $\mu\text{m}$   $\text{n}^+\text{In}_x\text{Al}_{1-x}\text{As}$  buffer layer with Si doping density of  $2 \times 10^{18}\text{cm}^{-3}$ , 1.5  $\mu\text{m}$   $\text{n}^-\text{In}_{0.83}\text{Ga}_{0.17}\text{As}$  absorption layer with Si doping concentration of  $3 \times 10^{16}\text{cm}^{-3}$  and 0.6  $\mu\text{m}$   $\text{p}^+\text{In}_{0.83}\text{Al}_{0.17}\text{As}$  cap layer with Be doping density of  $2 \times 10^{18}\text{cm}^{-3}$ . In order to provide the surface passivation,  $\text{SiN}_x$  film was deposited by ICPCVD (fabricated at 75  $^\circ\text{C}$ ) and PECVD technology (fabricated at 330  $^\circ\text{C}$ ) respectively. After that, Ohmic contacts were formed. The scheme of the detectors and the normalized response spectra of the detectors at room temperature are shown in Fig. 1. It is seen that the photo-responsivity extends up to 2.6 $\mu\text{m}$ , suggesting that the band gap energy of  $\text{In}_{0.83}\text{Ga}_{0.17}\text{As}$  layer is 0.48 eV at room temperature.

### 3. Results and discussion

Fig. 2 shows I-V characteristics at room temperature for two detectors with p-i-n area of 100 x 100  $\mu\text{m}^2$ . It is seen that the dark current of ICPCVD devices is significantly reduced comparing to PECVD devices. For mesa-structure

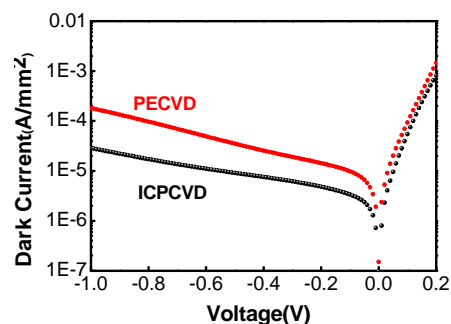


Fig.2 The current-voltage characteristics at room temperature for ICPCVD and PECVD devices.

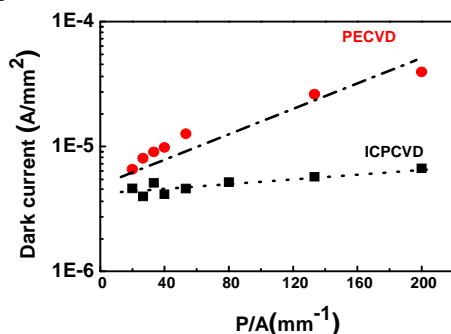


Fig.3 The dark current density at  $V_R = -0.1$  V as a function of the peripheral and area ratio (P/A) for ICPCVD and PECVD devices.

detectors, the dark current is the sum of the area dark current  $I_A$  and the perimeter dark current  $I_p$  due to the large surface state component. In order to identify the contribution of  $I_A$  and  $I_p$  to the dark currents, current–voltage (I–V) measurements were then performed on a set of detectors, with perimeter/area ( $P/A$ ) ratios varying between  $30 \text{ mm}^{-1}$  and  $200 \text{ mm}^{-1}$ . The results at  $V_R = -0.1 \text{ V}$  are shown in Fig.3. According to the equation:

$$J(V_R) = J_A(V_R) + J_p(V_R) \frac{P}{A} \quad (1)$$

The plot of  $J(V_R)$  versus  $P/A$  of equation (1) should produce a straight line with a slope equal to  $J_p(V_R)$  and y-intercept to  $J_A(V_R)$ . For both ICPCVD and PECVD devices, the obtained area current value  $J_A$  from the plot is

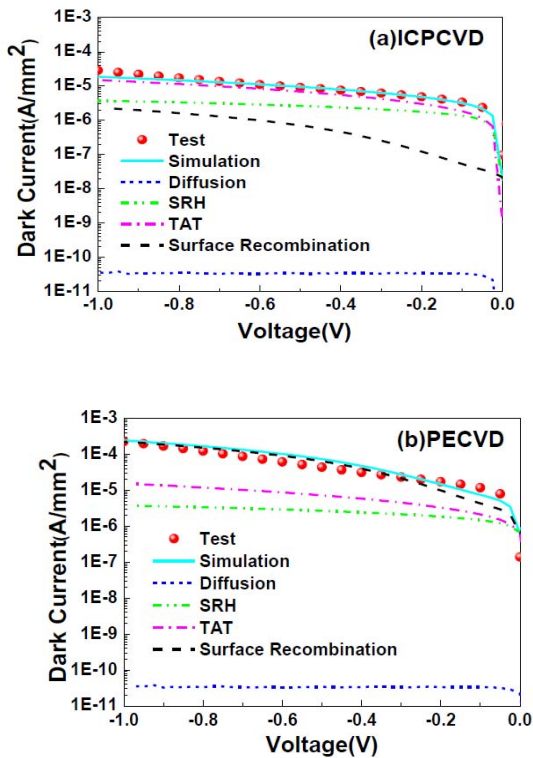


Fig.4 The experimental and simulated I–V curves at room temperature for (a) ICPCVD and (b) PECVD devices. The solid circles present the measured data while the solid and the dash lines are the simulated results and their four components, respectively. It is seen that TAT and SRH currents are the major contributors for the dark current at the low bias voltage for ICPCVD.

close to 100% of the dark current at  $V_R = -0.1 \text{ V}$  for ICPCVD devices in Fig.2; On the other hand,  $J_p$  is quite difference for two devices,  $2 \times 10^{-8} \text{ A/mm}$  for ICPCVD and  $2 \times 10^{-7} \text{ A/mm}$  for PECVD. Significant magnitude increase of  $J_p$  for PECVD informs a high surface current related to the mesa edge in the case.

To further quantitatively identify the surface currents contribution for two devices, I-V characteristic of the detectors is modeled and the device simulation is carried

out by Silvaco Atlas. In the low reverse bias range, the dark current can be described by four mechanisms: diffusion ( $I_{DIFF}$ ), SRH generation ( $I_{SRH}$ ), trap assisted tunneling ( $I_{TAT}$ ) and surface recombination ( $I_{S-R}$ ).

$$I_{TOTAL} = I_{DIFF} + I_{SRH} + I_{TAT} + I_{S-R} \quad (2)$$

In the TCAD simulation, one deep level trap near the middle band gap of InGaAs is selected acting as the recombination and trap center for SRH and TAT currents.

Fig. 4 shows the experimental and simulated I–V curves at room temperature. It is seen that Shockley-Read-Hall generation and trap-assisted tunneling currents are the principal components of dark current for ICPCVD devices while the surface recombination current is the large contributors for PECVD devices. The surface current for ICPCVD devices has two orders magnitude reduction comparing to PECVD devices. For the latter case, the low bias dark current components at various temperatures are listed in Table 1. It is clearly seen that even under the low temperature operation, the surface has a significant contribution to the dark current in PECVD devices. Based on these results, it is concluded that the major current of ICPCVD devices are due to SRH and TAT currents while the surface current, SRH current and TAT current dominate the dark current of PECVD devices.

Table 1 The dark current components under  $V_R = -0.05 \text{ V}$  at various temperatures for PECVD detectors

(A/mm <sup>2</sup> )	233 K	263 K	293 K	323 K
$I_{DIFF}$	$9.54 \times 10^{-13}$	$1.58 \times 10^{-12}$	$2.93 \times 10^{-11}$	$6.76 \times 10^{-10}$
$I_{TAT}$	$5.03 \times 10^{-8}$	$2.28 \times 10^{-7}$	$1.02 \times 10^{-6}$	$3.63 \times 10^{-6}$
$I_{SRH}$	$1.85 \times 10^{-8}$	$1.36 \times 10^{-7}$	$1.13 \times 10^{-6}$	$7.90 \times 10^{-6}$
$I_{S-R}$	$2.19 \times 10^{-8}$	$1.99 \times 10^{-7}$	$2.11 \times 10^{-6}$	$2.43 \times 10^{-5}$
$I_{TOTAL}$	$9.07 \times 10^{-8}$	$5.63 \times 10^{-7}$	$4.27 \times 10^{-6}$	$3.09 \times 10^{-5}$

#### 4. Conclusion

Two various surface passivation technologies were used to fabricate  $2.6 \mu\text{m}$  mesa InGaAs/InP p-i-n photodetectors. It is found that the dark current is significantly suppressed by using ICPCVD technology. A TCAD-based dark current model further reveals the dark current mechanisms in both ICPCVD and PECVD detectors.

#### Acknowledgements

This work was supported by 973 Program of China (No. 2012CB619200) and the open project of Key Laboratory of Infrared Imaging Materials and Detectors (IIMDKFJJ-12-06), Shanghai Institute of Technical Physics, Chinese Academy of Sciences.

#### References

- [1] R.Hoogeveen, et al, Infrared Phys. Technol. **42** (2001)1
- [2] Q.Kleipool, et al, Infrared Phys. Technol. **50**(2007)30 .
- [3] X. Ji, et al, J .Appl. Phys **114** (2013)224502.
- [4] P. Wei, Infrared Phys. Technol. **62** (2014)13.
- [5] Y.Zhang et al, Semicon. Sci. Technol. **23** (2008)125029.